Grațianite, $MnBi_2S_4$, a new mineral from the Băița Bihor skarn, Romania

Cristiana L. Ciobanu[1,*], Joël Brugger[2], Nigel J. Cook[1], Stuart J. Mills[3], Peter Elliott[2], Gheorghe Damian[4] and Floarea Damian[4]

[1]School of Earth and Environmental Sciences, University of Adelaide, North Terrace, Adelaide, SA 5005, Australia

[2]South Australian Museum, North Terrace, Adelaide, SA 5000, Australia

[3]Museum Victoria, Melbourne, P.O. Box 666, Melbourne, VIC 3001, Australia

[4]Technical University of Cluj Napoca, North University Center of Baia Mare, 62A Dr. Victor Babeş Street, 430083 Baia Mare, Romania

American Mineralogist

Revision 1: 7th January 2014

ABSTRACT

The new mineral grațianite, $MnBi_2S_4$, is described from the Băița Bihor skarn deposit, Bihor County, Romania. Grațianite occurs as thin lamellae, intimately intergrown with cosalite and bismuthinite, or as flower-shaped blebs within chalcopyrite, where it is associated with cosalite and tetradymite. Grațianite displays weak to modest bireflectance in air and oil, respectively, and strong anisotropy. The mean empirical composition based on 20 electron probe microanalyses is: $(Mn_{0.541}Fe_{0.319}Pb_{0.070}Cu_{0.040}Cd_{0.009}Ag_{0.001})_{\Sigma 0.980}(Bi_{1.975}Sb_{0.018})_{\Sigma 1.993}(S_{4.008}Se_{0.012}Te_{0.007})_{\Sigma 4.027}$, corresponding to the ideal formula $MnBi_2S_4$. Grațianite crystallizes in the monoclinic system (space group *C*2/*m*). Single crystal X-ray studies of material extracted by the Focused Ion Beam – Scanning

Electron Microscopy (FIB□SEM) technique, and carried out on the MX2 macromolecular beam line of the Australian Synchrotron determined the following cell dimensions: a = 12.6774(25) Å, b = 3.9140(8) Å, c = 14.7581(30) Å, β = 115.31(3)º, V = 662.0(2) Å^3 and Z = 4. The six strongest X-ray reflections and their relative intensities are: 3.448 Å (100), 2.731 Å (77), 2.855 Å (64), 3.637 Å (55), 3.644 Å (54) and 3.062 Å (51).

Grațianite is the monoclinic analogue of berthierite ($FeSb_2S_4$), garavellite [$Fe(Bi,Sb)_2S_4$] and clerite [$Mn(Sb,As)_2S_4$] (Nickel-Strunz class 02.HA.20). It is isostructural with synthetic sulfides and selenides in the $MnBi_2S_4$□$MnSb_2S_4$ and $MnBi_2Se_4$□$MnSb_2Se_4$ series, and with grumiplucite ($HgBi_2S_4$) and kudriavite, [$(Cd,Pb)Bi_2S_4$], ^{3}P members of the pavonite homologous series. The mineral is named for Grațian Cioflica (1927□2002), formerly Professor in Mineralogy and Ore Deposits at the University of Bucharest, Romania.

The Băița Bihor skarn, like others within the same belt, is geochemically complex. The availability of Cu, Zn and Pb, but also Ag, Bi, Mo and B, as well as a wide range of minor elements, has created an environment allowing for crystallization of an unusually diverse range of discrete minerals. Grațianite is part of the peculiar associations of Bi□Pb-sulfosalts and Bi-chalcogenides that are genetically related to Au-enrichment. This study demonstrates the versatility of FIB□SEM techniques for *in-situ* extraction of small volumes of well-characterized material, coupled with single crystal X-ray analysis using synchrotron radiation, for the characterization of new minerals.

Keywords: Grațianite, new mineral, Bismuth-manganese-sulfosalt, Băița Bihor, pavonite homologous series.

* Corresponding author. e-mail: Cristiana.ciobanu@adelaide.edu.au

INTRODUCTION

The new mineral grațianite, $MnBi_2S_4$, has been discovered in the Băița Bihor skarn deposit, Bihor County, Romania. The mineral is named for Grațian Cioflica (1927□2002), Professor in Mineralogy and Ore Deposits at the University of Bucharest, Romania, from 1968 until his formal retirement in 1994. During his career, Professor Cioflica worked extensively on the geology and mineralogy of the Upper Cretaceous 'banatite'-related ore deposits, as well as metallogenesis associated with Neogene volcanism. Prof. Cioflica published around 100 scientific papers on aspects of hydrothermal ore deposits and mineralogy, including several key papers on the Băița Bihor skarn (e.g., Cioflica and Vlad 1970, 1979; Cioflica et al. 1971, 1974, 1977, 1982, 1995). Particular emphasis was given to the conspicuous zoning of skarn ores and the deposit's diverse and unique skarn mineralogy, including the wide range of bismuth sulfosalt minerals in the deposit.

Type material consisting of one holotype specimen is deposited in the collection of the South Australian Museum, Adelaide, Australia, catalogue no. G33937. The mineral and name have both been approved by the IMA Commission on New Minerals and Mineral Names (IMA2013□076).

OCCURRENCE

The Northern Apuseni Mts., Romania represent the northernmost portion of the "Banatite" Magmatic and Metallogenic Belt (BMMB; Berza et al. 1998; Ciobanu et al. 2002), which extends southwards into eastern Serbia, then east into Bulgaria, and extends to the Pontides of northern Turkey and beyond.

The Băița metallogenic district is genetically related to a deep-seated Upper Cretaceous granitic pluton and defined by several bodies of skarn that host mineable concentrations of Cu, Pb, Zn, Mo, W, Bi, B, wollastonite and marble. The Băița Bihor Cu–Mo–Pb–Zn deposit (46° 28' 60" N, 22° 34' 60" E)

is the largest deposit in the district, with an estimated pre-mining size of 5 million tonnes of ore @ 0.56% Cu, 1.06% Zn, 0.46% Pb, 0.09% Mo; mining ceased in 2008.

The deposit consists of a dozen ore-pipes located some 1.2 to 1.5 km above a granitic batholith and hosted within a sequence of Triassic–Jurassic carbonate units (Cioflica and Vlad 1970; Cioflica et al. 1971, 1977, 1982; Stoici 1983; Ştefan et al. 1988; Ciobanu et al. 2002, Ilinca et al. 2012). There is a west-to-east metal zonation (Mo–Cu–Pb/Zn) across the ore-field, but each ore-pipe also features similar zonation trends from core to the skarn-marble contact, sometimes with superposition of discrete zones due to telescoping (Cioflica and Vlad 1970; Cioflica et al. 1971). Skarns range from calcic to magnesian and include wollastonite-, rhodonite-, garnet-, diopside-, humite-, phlogopite-, and vesuvianite-bearing sub-types. Wollastonite skarn is found at the margins of the orepipes adjacent to outer skarn-marble contacts. The deposit also features boron metasomatism represented by assemblages of ludwigite, kotoite, fluoborite and szaibélyite (Marincea 2000, 2001). Magmatic rocks and skarn phlogopite within the deposit district have been dated at about 76 Ma (Bleahu et al. 1984), and, recently, Re–Os molybdenite geochronology has provided an age of ~80 Ma for skarn mineralization (Zimmerman et al. 2008). Variation in the Re–Os molybdenite ages led Zimmerman et al. (2008) to propose a life span of as much as 2 My for fluid generation and mineralization.

Several mineral species have been first discovered at Băiţa Bihor (formerly Rézbánya). The deposit is type locality for hemimorphite (1853; although see Papp, 2004) and szaibélyite (1861), and most recently, for paděraite (Mumme and Žak 1985; Mumme 1986), makovickyite (Žak et al. 1994) and cuproneyite (Ilinca et al. 2012). Băiţa Bihor is also famous for its outstanding and often unique assemblages of Bi–Pb–(Ag)-sulfosalts, notably phases of the lillianite and pavonite homologous series, miharaite and a wide range of other species (e.g., Topa and Paar 2008; Topa et al. 2008; Ilinca et al. 2012).

Type material grațianite was extracted from a sample (BB71) collected in the upper part of the (Cu and diopside skarn-dominant) Antoniu orepipe at Băița Bihor by one of us (G.D.) in 1995, within a humite-diopside ± phlogopite skarn mineralized in Cu. The sample is part of a larger (2 kg) block housed at the North University Center of Baia Mare, Romania. Patches containing sulfosalts and tellurides attain a maximum size of 300 μm and occur within or at the boundaries between sulfides and skarn silicates (Fig. 1a). The mineral occurs as thin lamellae, intimately intergrown with cosalite and bismuthinite (Fig. 1b, c), or as flower-shaped blebs within chalcopyrite, where it is associated with cosalite and minor tetradymite (Fig. 1d, e). Other minerals observed in the same sample include aikinite and pavonite (minor), and various members of the tetradymite homologous series (Cook et al. 2007a; Ciobanu et al. 2009a), including tetradymite, aleksite and unnamed $PbBi_4Te_4S_3$ (Cook et al. 2007b). Minute inclusions of native gold are observed within grațianite (Fig. 1c). Other mineral species noted within the same hand sample include: aikinite, pavonite, felbertalite, wittichenite, chalcopyrite, minor bornite, galena, sphalerite, molybdenite, hessite and cervelleite.

Type grațianite occurs as lamellae, no more than 20 μm in width, within cosalite and bismuthinite, and intergrown with cosalite as bleb-like inclusions enclosed within coarse-grained chalcopyrite (Fig. 1). No twinning is observed. A preliminary description of grațianite, as an unnamed mineral, was given by Damian et al. (2004). Grațianite has not been observed macroscopically.

PHYSICAL AND OPTICAL PROPERTIES

Color (macroscopic), streak, luster, hardness, cleavage, fracture and parting could not be observed due to the size of the mineral in the type material. Density could not be measured because of insufficient material. The calculated density is 6.031 g cm^{-3} based on the empirical formula (see below).

Grațianite is medium grey in reflected light, with slightly lower reflectance than coexisting cosalite. The mineral displays moderate bireflectance in air (Fig. 1d) and strong bireflectance (with bluish and brownish tints) in oil immersion. Grațianite displays strong anisotropy (shades of grey with distinct purple and brown tints; Fig. 1e). No internal reflections are noted. Due to the small size of the grains within the type material, and the fact that these are intimately intergrown with cosalite, no reflectance data have been obtained for grațianite.

CHEMICAL COMPOSITION

Quantitative analyses were performed at Adelaide Microscopy, University of Adelaide, on a Cameca SX-51 electron microprobe with four wavelength-dispersive spectrometers. Analytical conditions were: 20 kV accelerating voltage, 20 nA beam current and a beam diameter of 2 μm.

Results of electron probe microanalysis are summarized, together with the standards used, in Table 1; no other elements were detected other than those listed. The mean empirical composition (20 spot analyses) calculated on the basis of 7 atoms per formula unit is $(Mn_{0.541}Fe_{0.319}Pb_{0.070}Cu_{0.040}Cd_{0.009}Ag_{0.001})_{\Sigma 0.980}(Bi_{1.975}Sb_{0.018})_{\Sigma 1.993}(S_{4.008}Se_{0.012}Te_{0.007})_{\Sigma 4.027}$. This gives the simplified structural formula $MnBi_2S_4$, corresponding to 9.14 wt.% Mn, 69.53 wt.% Bi, 21.33 wt.%, total 100 wt%.

CRYSTAL STRUCTURE

Microsampling

The small and intergrown character of grațianite in the type specimen necessitated an appropriate method to obtain material for crystal structure determination. A wedge-shaped piece of grațianite, approximately 40 x 20 x 10 μm in size, was extracted from the surface of a polished mounted ore

section using a Focused Ion Beam – Scanning Electron Microscope (FIB□SEM) (Fig. 2). A Helios nanolab platform (Adelaide Microscopy) was used, following procedures outlined by Ciobanu et al. (2011).

Single crystal study

Single-crystal X-ray studies were carried out on the MX2 macromolecular beam line of the Australian Synchrotron. Data were collected at room temperature using an ADSC Quantum 315r detector using monochromatic radiation with a wavelength of 0.7100 Å. A φ scan was employed with frame widths of 1º and a counting time per frame of 1 s. The intensity data sets were processed using XDSauto and SADABS. Several atoms were first found using SHELXS-97 (Sheldrick, 2008), followed by the location of all other atoms via subsequent difference-Fourier syntheses during the refinement, performed using SHELXL-97 (Sheldrick, 2008). Neutral scattering factors from the International Tables Vol. C (Tables 4.2.6.8 and 6.1.1.4) were used in the refinement (Wilson, 1992). The Bi1 and Bi2 sites refined to full occupancy and were fixed throughout the refinement. The Mn3 site refined to 1.39 occupancy in the initial stages, while the Mn4 site also refined to full occupancy. It was therefore decided to leave the Mn4 site at full occupancy and apportion the remaining metals in the Mn3 site on the basis of the microprobe analyses. It is possible that there is a distribution of metals on both sites; however, given that there are a number of metals found in grațianite, it is impossible to test this theory. It should be noted that attempts to add heavy metals (and Mn:Fe on both sites) in the Mn4 site resulted in an unstable refinement. The final model, with all atoms refined anisotropically, converged to R_1 = 10.35% for 878 reflections with $F_o > 4\sigma(F)$.

Grațianite crystallizes in the monoclinic system (space group *C*2/*m*). Cell parameters from the single crystal study are: a = 12.6774(25) Å, b = 3.9140(8) Å, c = 14.7581(30) Å, β = 115.31(3)º, V = 662.0(2) Å^3 and Z = 4. The a:b:c ratios calculated from the single crystal unit-cell parameters are

3.2389:1:3.7706. Data collection and refinement details are given in Table 2, atom coordinates and displacement parameters in Table 3, and selected bond distances in Table 4.

The crystal structure of grațianite is equivalent to that of synthetic $MnBi_2S_4$ (Lee et al. 1993). The structure (Fig. 3) is a member of the family of structures that have glide plane-twinned cubic closest packed arrangements based on that of NaCl. The structure consists of distorted BiS_{3+3} octahedra, corner and edge-shared with MnS_6 octahedra. Lee et al. (1993) note that as Bi increases, the β angle similarly increases, from 115 ° to almost 117 °. The β angle for grațianite of 115.31(3)º, is consistent with a composition which equates to close-to-end-member composition, or in the case of grațianite, with Bi ~ 2.0 apfu. X-ray powder diffraction data could not be recorded due to the nature of the intergrowths and the size of the crystal extracted by FIB□SEM. Attempts to collect data using a desktop diffractometer gave no useful data (Oxford Diffraction Xcalibur E diffractometer equipped with an Eos CCD detector; Mo-K*a* X-radiation; detector distance of 45.53 mm). The powder pattern of grațianite was calculated using CrystalDiffract for Cu $K\alpha_1$ (λ = 1.54050 Å). The six strongest X-ray reflections and their relative intensities are: 3.448 Å (100), 2.731 Å (77), 2.855 Å (64), 3.637 Å (55), 3.644 Å (54) and 3.062 Å (51). The X-ray powder diffraction data are given in Table 5.

DISCUSSION

Comparison with related species

Grațianite is a monoclinic analogue of berthierite ($FeSb_2S_4$; Buerger and Hahn 1955; Lemoine et al. 1991), garavellite ($Fe(Bi,Sb)_2S_4$; Gregorio et al. 1979; Bindi and Menchetti 2005) and clerite ($Mn(Sb,As)_2S_4$; Murzin et al. 1996; Bente and Edenharter 1989, 1990). Berthierite, garavellite and clerite minerals comprise the berthierite isotypic series of Moëlo et al. (2008) (Nickel-Strunz class

187 02.HA.20). Bindi and Menchetti (2005) showed that, in garavellite, the Sb and Bi atoms are positioned
188 at distinct sites, confirming that garavellite is not simply a Bi-rich variety of berthierite.

189 Dimorphism is recognized in the class; clerite, for example, is the dimorph of synthetic monoclinic
190 $MnSb_2S_4$ synthesized by Pfitzner and Kurowski (2000) and earlier reported as an unnamed phase by
191 Harris (1989). Compounds in the continuous solid solution series $MnBi_2S_4$–$MnSb_2S_4$ and analogue
192 selenide $MnBi_2Se_4$–$MnSb_2Se_4$ series have been experimentally prepared (Lee et al. 1993; Kurowski
193 2003; Lecker 2011), with a view to determining the potentially useful magnetic and electric properties
194 of sulfides and selenides with the general formula $MnPn_2Q_4$ (*Pn* = Sb or Bi; *Q* = S or Se). Lee et al.
195 (1993) also prepared non-stoichiometric compounds ($Mn_{1-x}Bi_{2+y}S_4$ and $Mn_{1-x}Bi_{2+y}Se_4$) with extended
196 defect structures and argued for the presence of compounds with varied stoichiometry in the system
197 MnS-Bi_2S_3 controlled by specific zigzag line segments and point defects. Lecker (2011) also showed
198 incomplete solid solution between $MnBi_2S_4$ and $MnSb_2S_4$. Taking the formula $Mn(Sb_{2-x}Bi_x)_2S_4$, there is
199 a miscibility gap between values of $x = 0.4$ and 1.0.

200 Experimental studies of the quaternary system MnS–FeS–Sb_2S_3–Bi_2S_3 are required to adequately
201 understand the reasons for the observed distribution of structural types relative to chemistry,
202 particularly between Bi- and Sb-bearing phases. The key question of whether polymorphism extends
203 across the entire group remains open. Controls on the distribution of structures in natural samples may
204 include pressure since Pfitzner and Kurowski (2000) observed a pressure-dependent, reversible
205 reaction from the monoclinic (*mC*28) to orthorhombic (*oP*28) modification of the $MnSb_2S_4$ phase
206 above 3 GPa and 1073 K, which reverted to the monoclinic form after one week at 763 K.

207 The bond lengths for grațianite are consistent with those reported by Lee et al. (1993) for
208 $Mn_{0.7}Bi_{2.2}S_4$, where <Bi1–O>, <Bi2–O>, and <Mn4–O> are 2.823, 2.818 and 2.631 Å for grațianite,
209 compared to 2.822, 2.780 and 2.640 Å, respectively for $Mn_{0.7}Bi_{2.2}S_4$. The <Mn3–O> site which
210 contains substantial Fe in grațianite, has a slightly shorter average bond length (2.591 Å) than Mn4, but

is longer than the same site in garavellite (2.536 Å; Bindi and Menchetti 2005). This probably reflects the multi-anion nature of the site incorporating Pb, Cu and Cd.

Grațianite and the compounds with monoclinic *C*2/*m* structures synthesized by Lee et al. (1993), Pfitzner and Kurowski (2000), Kurowski (2003) and Lecker (2011) are isostructural with $HgBi_2S_4$ (Mumme and Watts 1980), later discovered and named as the mineral grumiplucite (Orlandi et al. 1998). Kurowski (2003) noted, however, that structural variations among the monoclinic *C*2/*m* Mn-(Fe) □Bi□Sb-chalcogenides show "quasi-isotypic relationships". Synthetic $MnBi_2S_4$ is perfectly isotypic with $MnSb_2Se_4$, $MnBi_2Se_4$ and $FeSb_2Se_4$ but not with $HgBi_2S_4$ or $MnSb_2S_4$. This is a response to the readily distorted character of the layered compounds in which the layers are held together only by weak Van-der-Waals forces, also explaining the aforementioned miscibility gap in the $MnSb_{2-x}Bi_xS_4$ series (Lecker 2011). Complications brought about by such structural distortion (Lee et al. 1993; Djieutedjeu et al. 2010) are compounded by the tendency for development of mixed Mn/Bi sites in the Mn□Bi-chalcogenides (Lee et al. 1993; Kurowski 2003; Lecker 2011) due to the similar size of the Mn^{2+} and Bi^{3+} ions (0.97 and 1.03 Å, respectively; Shannon 1976). Mixed sites are less likely in the Sb-analogues due to the far smaller Sb^{3+} ion (0.76 Å; Shannon 1976). Lecker (2011) provides a detailed treatment of occupancy in the Mn-sites in the analogue $MnSb_{2-x}Bi_xSe_4$ compounds. An added complication for grațianite is the presence not only of significant Fe but also minor Pb, Cu and Cd.

Grumiplucite, along with kudriavite, [$(Cd,Pb)Bi_2S_4$; Chaplygin et al. 2005, Balić-Žunić and Makovicky 2007] is a ^{3}P member of the pavonite homologous series (Makovicky et al. 1977; Perez-Mato et al. 2013). Structurally, therefore, grațianite is a new natural ^{3}P homologue within the pavonite homologous series. Chemically, however, the new mineral represents the first naturally occurring monoclinic dimorph of minerals in the berthierite polytypic series. Comparative crystal structural data for minerals and selected synthetic compounds in both the berthierite isotypic group and ^{3}P pavonite homologues are summarized in Table 6.

235

236 **Grațianite in the context of skarn formation**

237 The appearance and morphology of grațianite in the type material, in particularly the intimate
238 association with cosalite, is suggestive of co-crystallization of grațianite and cosalite, or of exsolution
239 from cosalite or a higher-temperature precursor phase. Only a few Mn-bearing sulfosalt minerals are
240 currently known (Moëlo et al. 2008), and Mn would appear not to be readily incorporated in most
241 common sulfosalt series (cosalite, bismuthinite derivatives, lillianite or pavonite homologous series).
242 Exceptions include the tetrahedrite isotypic series, the andorite series in which the exchange $Pb^{2+} \leftrightarrow$
243 $(Mn, Fe, Cd)^{2+}$ is recognized (e.g., in ramdohrite and uchucchacuaite), the $Mn^{2+} \leftrightarrow Fe^{2+}$ exchange in
244 jamesonite–benavidesite (Chang et al. 1987; Moëlo et al. 2008), and the recently described additional
245 member of the lillianite homologous series, menchettiite (Bindi et al. 2012).

246 Stability relationships in the system Mn□Bi□S are poorly constrained even though a number of
247 experimental studies give some inferences about temperature stabilities. Kurowski (2003) gives the
248 experimental and thermodynamically-derived melting point for synthetic $MnBi_2S_4$ as 750 °C and 809
249 °C, respectively. Pfitzner and Kurowski (2000) were able to synthesize monoclinic $MnSb_2S_4$ by solid
250 state reaction of MnS and Sb_2S_3 at 500 °C. Data given by Barton (1971) and references therein indicate
251 stability of analogue berthierite up to at least around 500□550 °C.

252 Considering such temperature ranges, formation of grațianite and associated Bi-sulfosalt and
253 (sulfo)-tellurides at Băița Bihor is most likely to be part of the Cu-ore deposition during prograde skarn
254 formation. This has been also inferred from textural relationships between ore and skarn minerals
255 (Damian et al. 2004). Gold enrichment in skarn deposits, both here and in skarn deposits elsewhere, is
256 genetically linked to associations of Bi-sulfosalts and tellurides (e.g., Meinert 2000; Ciobanu et al.
257 2009b).

258

259 # IMPLICATIONS

260

261 The Băița Bihor skarn is a particularly complex deposit from a geochemical perspective. The
262 availability of Cu, Zn and Pb, but also Ag, Bi, Mo and B, as well as a wide range of minor elements
263 (Se, Te, Co, In, Sb, Sn and W) at significant concentrations has created an environment allowing for
264 crystallization of an unusually diverse range of discrete minerals (see also Szakall 2002, Papp 2004).
265 The wide variation in skarn types has also led to many of these species having restricted distribution.
266 Until now, relatively few Mn-bearing minerals have been noted from the locality. Others are
267 predictable to be discovered in Au□Bi-bearing associations.

268 In addition to the diverse and unusual mineralogy of the mineralized skarns, the concentrations of a
269 wide range of trace elements incorporated within common sulfides at Băița Bihor are also unusually
270 high. This has been demonstrated for sphalerite (Cook et al. 2009), bornite (Cook et al. 2011), and
271 galena (George et al. in review). Bornite and galena from Băița Bihor are both significant carriers of
272 Ag and Bi, whereas sphalerite contains significant In and Co.

273 Grațianite is part of the peculiar Bi-mineral associations tied to Au-enrichment in skarns at Băița
274 Bihor and worldwide. Ciobanu et al. (2009b) have shown that some Bi□Pb-sulfosalts and Bi-
275 chalcogenides at Băița Bihor are significant carriers of Au. Combining investigation by FIB□SEM,
276 TEM imaging and electron diffraction and High-Angle Annular Dark Field – Scanning Transmission
277 Electron Microscopy mapping, Ciobanu et al. (2011) have addressed the nano- to micron-scale
278 character of symplectites containing Ag-substituted heyrovskýite, berryite, aikinite and galena from
279 Zn□Pb ore in skarn at Băița Bihor and how trails of fine particles of Au-bearing hessite form during
280 retrograde replacement of one sulfosalt (in this case heyrovskýite) by another.

281 Many of the mineral deposits within the BMMB display a conspicuous Bi–Ag–Sn–Co□Te–Se–Au
282 trace geochemical signature (Ciobanu et al. 2002). The skarn deposits within this belt appear

283 particularly well endowed with a number of minor elements, notably bismuth. The complex, widely
284 varying and intergrown character of the Băița Bihor ores, as well as the extremely complex
285 mineralogical distributions of many elements, continue to provide considerable interest for
286 mineralogists and for researchers aiming to understand ore formation in a polymetallic system. This
287 same complexity nevertheless presented major challenges for ore processing during the lifetime of the
288 mine.

289 The determination of the grațianite structure in this study has demonstrated the value of FIB□SEM
290 techniques for *in-situ* extraction of small volumes of well-characterized material from the surface of a
291 polished section for single crystal X-ray analysis using synchrotron radiation. Such an approach can be
292 useful for characterization of other potential new mineral species only present in minute quantities in
293 complex samples. Because it is an *in-situ* method, it has great value for linking mineralogy to mineral
294 reactions and ore genesis at an appropriate scale.

295

296 **ACKNOWLEDGEMENTS**

297 We acknowledge the support of AMMRF for access to FIB□SEM facilities. Jason Price from the
298 Australian Synchrotron is thanked for help with processing the data. Chairman Peter Williams and
299 members of IMA-CNMMN are gratefully acknowledged for feedback. Angus Netting and Leonard
300 Green (Adelaide Microscopy) assisted with Electron Probe Microanalysis and FIB□SEM operation,
301 respectively. CLC, NJC and GD kindly thank S.C. Băița Bihor S.A. for access to the Băița Bihor mine
302 on a number of occasions between 2000 and 2008. Last but not least we gratefully acknowledge the
303 helpful comments of reviewers Luca Bindi and Klaus Bente, as well as those of American Mineralogist
304 Associate Editor Joshua Feinberg. This is TRaX contribution no. XXX.

305

306

REFERENCES CITED

Balić-Žunić, T., and Makovicky, E. (2007) The crystal structure of kudriavite, (Cd, Pb)Bi_2S_4. Canadian Mineralogist, 45, 437–443.

Barton, P.B., Jr. (1971) The Fe–Sb–S system. Economic Geology, 66, 121–132.

Bente, K., and Edenharter, A. (1989) Rontgenographische strukturanalyse von $MnSb_2S_4$ und strukturverfeinerung von berthierit, $FeSb_2S_4$. Zeitschrift für Kristallographie, 185, 31–33.

Bente, K., and Edenharter, A. (1990) X-ray structure analysis of synthetic $MnSb_2S_4$ and structure refinement of natural $FeSb_2S_4$ (berthierite). Zeitschrift für Kristallographie, suppl. 2, 36.

Berza, T., Constantinescu, E., and Vlad, Ş.N. (1998) Upper Cretaceous magmatic series and associated mineralisation in the Carpathian–Balkan orogen. Resource Geology, 48, 291–306.

Bindi, L., and Menchetti, S. (2005) Garavellite, $FeSbBiS_4$, from the Caspari mine, North Rhine-Westphalia, Germany: composition, physical properties and determination of the crystal structure. Mineralogy and Petrology, 85, 131–139.

Bindi, L., Keutsch, F.N., and Bonazzi, P. (2012) Menchettiite, $AgPb_{2.40}Mn_{1.60}Sb_3As_2S_{12}$, a new sulfosalt belonging to the lillianite series from the Uchucchacua polymetallic deposit, Lima Department, Peru. American Mineralogist, 97, 440–446.

Bleahu, M., Soroiu, M., and Catilina, R. (1984) On the Cretaceous tectonic-magmatic evolution of the Apuseni Mountains as revealed by K–Ar dating. Revue Roumaine de Physique, 29, 123–130.

Buerger, M.J., and Hahn, T. (1955) The crystal structure of berthierite, $FeSb_2S_4$. American Mineralogist, 40, 226–238.

Chang, L.L.Y., Li, X., and Zheng, C. (1987) The jamesonite–benavidesite series. Canadian Mineralogist, 25, 667–672.

Chaplygin, I.V., Mozgova, N.N., Magazina, L.O., Kuznetsova, O.Yu., Safonov, Yu.G., Bryzgalov, I.A., Makovicky, E., and Balić-Žunić, T. (2005) Kudriavite, (Cd, Pb)Bi_2S_4, a new mineral species from Kudriavy volcano, Iturup island, Kurile arc, Russia. Canadian Mineralogist, 43, 695–701.

Ciobanu, C.L., Cook, N.J., and Stein, H. (2002) Regional setting and geochronology of the Late Cretaceous Banatitic Magmatic and Metallogenic Belt. Mineralium Deposita, 37, 541–567.

Ciobanu, C.L., Pring, A., Cook, N.J., Self, P., Jefferson, D., Dima, G., and Melnikov, V. (2009a) Chemical-structural modularity in the tetradymite group: a HRTEM study. American Mineralogist, 94, 517–534.

Ciobanu, C.L., Cook, N.J., Pring, A., Brugger, J., Danushevsky, L., and Shimizu, M. (2009b) 'Invisible gold' in bismuth chalcogenides. Geochimica et Cosmochimica Acta, 73, 1970–1999.

Ciobanu, C.L., Cook, N.J., Utsunomiya, S., Pring, A., and Green, L. (2011): Focussed ion beam - transmission electron microscopy applications in ore mineralogy: bridging micron- and nanoscale observations. Ore Geology Reviews, 42, 6–31.

Cioflica, G., and Vlad, Ş.N. (1970) La nature polyascendante des métasomatites laramiques de Băiţa Bihorului (Monts Apuseni). Acta Geologica Academiae Scientiarum Hungaricae, 14, 135–141.

Cioflica, G., and Vlad, Ş.N. (1979) Bi-sulfosalts related to Laramian skarns of the Bihor Mountains (Northern Apuseni Mountains). Revue Roumaine de Géologie, Géophysique, Géographie, Serie Géologie, 23, 15–21.

Cioflica, G., Vlad, S., and Stoici, S. (1971) Répartition de la minéralisation dans les skarns de Băiţa Bihorului. Revue Roumaine de Géologie, Géophysique, Géographie, Serie Géologie, 15, 43–58.

Cioflica, G., Vlad, S., Iosof, D. and Panican, A. (1974) Thermal and metasomaatic metamorphism of the Paleozoic rocks belonging to the Arieseni Unit (Băiţa Bihorului). Studii şi Cercetare Géologie Géofizică şi Géographie, Serie Géologie, 19, 43–68.

Cioflica, G., Vlad, S., Volanschi, E., and Stoici S. (1977) Magnesian skarns and associated mineralization at Băiţa Bihor. Studii şi Cercetare Géologie Géofizică şi Géographie, Serie Géologie, 22, 39–57. (in Romanian).

Cioflica, G., Berbeleac, I., Lazăr, C., Ştefan, A., and Vlad, Ş.N. (1982) Metallogeny related to Laramian magmatism in the Bihor Mts. (northern Carpathians, Romania). Analele Universităţii din Bucureşti, vol. XXXI, 3–12.

Cioflica, G., Jude, R., Lupulescu, M., Simon, G., and Damian G. (1995) New data on the Bi-minerals from the mineralizations related to Paleocene magmatites in Romania. Romanian Journal of Mineralogy, 76, 9–23.

Cook, N.J., Ciobanu, C.L., Wagner, T., and Stanley, C.J. (2007a) Minerals of the system Bi-Te-Se-S related to the tetradymite archetype: review of classification and compositional variation. Canadian Mineralogist, 45, 665–708.

Cook, N.J., Ciobanu, C.L., Stanley, C.J., Paar, W., and Sundblad, K. (2007b) Compositional data for Bi-Pb tellurosulfides. Canadian Mineralogist, 45, 417–435.

Cook, N.J., Ciobanu, C.L., Pring, A., Skinner, W., Danyushevsky, L., Shimizu, M., Saini-Eidukat, B., and Melcher, F. (2009) Trace and minor elements in sphalerite: a LA-ICP-MS study. Geochimica et Cosmochimica Acta, 73, 4761–4791.

Cook, N.J., Ciobanu, C.L., Danyushevsky, L.V., and Gilbert, S. (2011) Minor elements in bornite and associated Cu-(Fe)-sulfides: a LA-ICPMS study. Geochimica et Cosmochimica Acta, 73, 4761–4791.

Damian, F., Ciobanu, C.L., Cook, N.J., and Damian, G. (2004) Lead-bismuth sulphotellurides and associated minerals in the Upper Cretaceous Băiţa Bihor Cu-(Mo) skarn, North Apuseni Mts., Romania. In: Gold-Silver-Telluride Deposits of the Golden Quadrilateral, South Apuseni Mts., Romania (Ciobanu, C.L. and Cook, N.J., eds.). Guidebook, International Field Workshop of IGCP-

486, Alba Iulia, Romania, 31st August–7th September 2004. IAGOD Guidebook Series vol. 12, p. 221–224.

Djieutedjeu, H., Poudeu, P.F.P., Takas, N.J., Makongo, J.P.A., Rotaru, A., Ranmohotti, K.G.S., Anglin, C.J., Spinu, L., Wiley, J.B. (2010) Structural-distortion-driven cooperative magnetic and semiconductor-to-insulator transitions in ferromagnetic $FeSb_2Se_4$. Angewandte Chemie International Edition, 49, 9977–9981.

George, L., Cook, N.J., and Ciobanu, C.L. (in review) Trace and minor elements in galena: A reconnaissance LA-ICP-MS study. American Mineralogist.

Gregorio, F., Lattanzi, P., Tanelli, G., and Vurro, F. (1979) Garavellite, $FeSbBiS_4$,a new mineral from the Cu–Fe deposit of Valle del Frigido in the Apuane Alps, northern Tuscany, Italy. Mineralogical Magazine, 43, 99–102.

Harris, D.C. (1989) The mineralogy and geochemistry of the Hemlo gold deposit, Ontario. Geological Survey of Canada, Economic Geology Report 38, 88 pp.

Ilinca, G., Makovicky, E., Topa, D., and Zagler, G. (2012) Cuproneyite, $Cu_7Pb_{27}Bi_{25}S_{68}$, a new mineral species from Băița Bihor, Romania. Canadian Mineralogist, 50, 353–370.

Kurowski, D. (2003) Mangan-Chalkogenometallate der 15. Gruppe und binäre Kupfertelluride. Unpublished Ph.D. thesis, University of Regensberg, Germany, 175 pp.

Lecker, A. (2011) Synthese, Strukturchemie und physikalische Untersuchungen an Mangan-, Eisen- und Quecksilber-Chalkogenometallatverbindungen. Unpublished Ph.D. thesis, University of Regensberg, Germany, 204 pp.

Lee, S., Fischer, E., Czerniak, J., and Nagasundaram, N. (1993) Synthesis and structure of two phases with both extended and point defects: $Mn_{1-x}Bi_{2+y}S_4$ and $Mn_{1-x}Bi_{2+y}Se_4$. Journal of Alloys and Compounds, 197, 1–5.

399 Lemoine, P., Carré, D., and Robert, F. (1991) Structure du sulfure de fer et d'antimoine, $FeSb_2S_4$
400 (berthiérite). Acta Crystallographica, C47, 938–940.
401 Makovicky, E., Mumme, W.G., and Watts, J.A. (1977) The crystal structure of synthetic pavonite,
402 $AgBi_3S_5$, and the definition of the pavonite homologous series. Canadian Mineralogist, 15, 339–348.
403 Marincea, Ş. (2000) Fluoborite in magnesian skarns from Băiţa Bihor (Bihor Massif, Apuseni
404 Mountains, Romania). Neues Jahrbuch für Mineralogie Monatshefte, 357–371.
405 Marincea, S. (2001) New data on szaibelyite from the type locality, Băiţa Bihor. Canadian
406 Mineralogist, 39, 111–127.
407 Meinert, L.D. (2000) Gold in skarns related to epizonal intrusions. Reviews in Economic Geology, 13,
408 347–375.
409 Moëlo, Y., Makovicky, E., Mozgova, N.N., Jambor, J.L., Cook, N.J., Pring, A., Paar, W., Nickel, E.H.,
410 Graeser, G., Karup-Møller, S., Balić-Žunić, T., Mumme, W.G., Vurro, V., Topa, D., Bindi, L.,
411 Bente, K., and Shimizu, M. (2008) Sulfosalt systematics: a review. Report of the Sulfosalt Sub-
412 committee of the IMA Commission on Ore Mineralogy. European Journal of Mineralogy, 20, 7–46.
413 Mumme, W.G. (1986) The crystal structure of paderaite, a mineral of the cuprobismutite series. The
414 Canadian Mineralogist, 24, 513–521.
415 Mumme, W.G., and Watts, J.A. (1980) $HgBi_2S_4$: Crystal structure and relationship with the pavonite
416 homologous series. Acta Crystallographica, B36, 1300–1304.
417 Mumme, W.G., and Žák, K. (1985) Paděraite, $Cu_{5.9}Ag_{1.3}Pb_{1.6}Bi_{11.2}S_{22}$, a new mineral of the
418 cuprobismutite–hodrushite group. Neues Jahrbuch für Mineralogie Monatsheft, 557–567.
419 Murzin, V.V., Bushmakin, A.F., Sustavov, S.G., and Shcherbachev, D.K. (1996). Clerite $MnSb_2S_4$ – a
420 new mineral from the Vorontsovskoye gold deposit in the Urals. Zapiski Vses. Mineral. Obshch.,
421 125, 95–101 (in Russian with English abstract).

Orlandi, P., Dini, A., and Olmi, F. (1998) Grumiplucite, a new mercury–bismuth sulfosalt species from the Levigliani mine, Apuan Alps, Tuscany, Italy. Canadian Mineralogist, 36, 1321–1326.

Papp, G. (2004) History of Minerals, Rocks and Fossil Resins Discovered in the Carpathian Region. Studia Naturalia 15, Hungarian Natural History Museum, Budapest, 216 pp.

Perez-Mato J.M., Elcoro, L., Makovicky, E., Topa, D., Petříček, V., and Madariaga, G. (2013) Conspicuous variation of the lattice unit cell in the pavonite homologous series and its relation with cation/anion occupational modulations. Materials Research Bulletin, 48, 2166–2174.

Pfitzner, A. and Kurowski, D. (2000). A new modification of $MnSb_2S_4$ crystallizing in the $HgBi_2S_4$ structure type. Zeitschrift für Kristallographie – Crystalline Materials, 215, 373–376.

Shannon, R.D. (1976) Revised effective ionic radii and systematic studies of interatomic distances in halides and chalcogenides. Acta Crystallographica, A32, 751–767.

Sheldrick, G.M. (2008) A short history of *SHELX*. Acta Crystallographica, A64, 112–122.

Ştefan, A., Lazăr, C., Berbeleac, I., and Udubaşa, G. (1988) Evolution of the banatitic magmatism in the Apuseni Mts. and associated metallogenesis. Dări de Seamă ale Şedinţelor Institutului de Geologie şi Geofizică, 72–73, 195–213.

Stoici, S.D. (1983) Districtul metalogenetic Băiţa Bihorului. Editura Academiei Republicii Socialiste România, Bucharest, 183 pp. (in Romanian).

Szakall, S., ed. (2002) Minerals of the Carpathians. Granite Publishing House Ltd., Czech Republic, 480 pp.

Topa, D., and Paar, W.H. (2008) Cupromakovickyite, $Cu_8Pb_4Ag_2Bi_{18}S_{36}$, a new mineral of the pavonite homologous series. Canadian Mineralogist, 46, 503–514.

Topa D., Makovicky E., and Balić-Žunić, T. (2008) What is the reason of the doubled unit cell volumes of copper–lead rich pavonite homologues? The crystal structures of cupromakovickyite and makovickyite. Canadian Mineralogist, 46, 515–523.

Wilson, A.J.C., Ed. (1992) International Tables for Crystallography: Mathematical, Physical, and Chemical Tables, volume 3. Published for the International Union of Crystallography by Kluwer Academic Publishers.

Žak, L., Frýda, J., Mumme, W.G., and Paar, W.H. (1994) Makovickyite, $Ag_{1.5}Bi_{5.5}S_9$ from Băiţa Bihorului, Romania: the ^{4}P natural mineral member of the pavonite series. Neues Jahrbuch für Mineralogie Abhandlungen, 168, 147–169.

Zimmerman, A., Stein, H.J., Hannah, J.L., Kozelj, D., Bogdanov, K., and Berza, T. (2008). Tectonic configuration of the Apuseni-Banat-Timok-Srednogorie belt, Balkans-South Carpathians, constrained by high precision Re-Os molybdenite ages. Mineralium Deposita, 43, 1–21.

Figure captions

Figure 1. Typical occurrence and association of grațianite within the copper ore at Băița Bihor. Location of patches imaged in b-e are circled on (a). Optical image (reflected light), illustrating the occurrence of type grațianite within composite sulphosalt-telluride inclusions in chalcopyrite (Cp); minor sphalerite (Sp) present. (b) Back-scattered electron image (BSE) showing lamellar grațianite (Gr) intergrown with cosalite (Cos) and bismuthinite (Bism). (c) BSE image showing a detail within a composite patch of grațianite (Gr) and cosalite (Cos) in which grațianite hosts inclusions of native gold (Au). (d and e) Optical images (reflected light, normal and half-crossed polars, respectively) showing the bireflectance and birefringence colours of gratianite (Gr) comparatively to cosalite (Cos) and emphasizing the strong anisotropy of grațianite. Ttd = tetradymite.

Figure 2. FIB-SEM procedure used to extract material for crystal structure determination (a) BSE image of the Bi-sulfosalt patch containing grațianite (shown in figure 1d, e) from which a slice was extracted for single crystal X-ray study. (b-e) Secondary-electron images showing details of extraction (b), lifting-transporting (c-d), and mounting of the slice on a tungsten stub (e). For the single crystal X-ray study, the synchrotron beam was placed on the flat surface on top of the grain. Abbreviations as in figure 1.

Figure 3. Grațianite structure. BiS_{3+3} distorted octahedral are shown in green, MnS_6 octahedra in mauve.

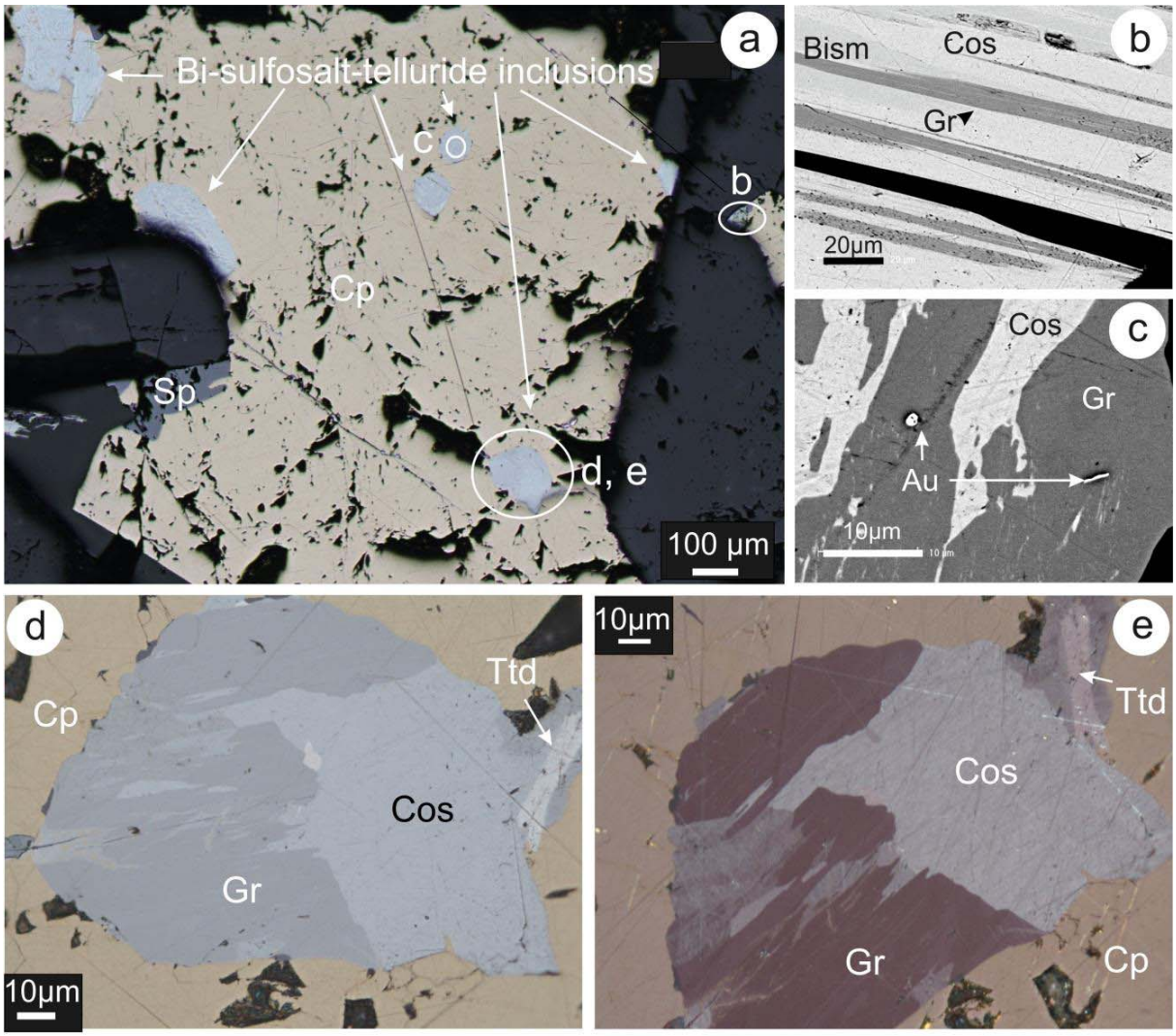

Ciobanu et al. Figure 1

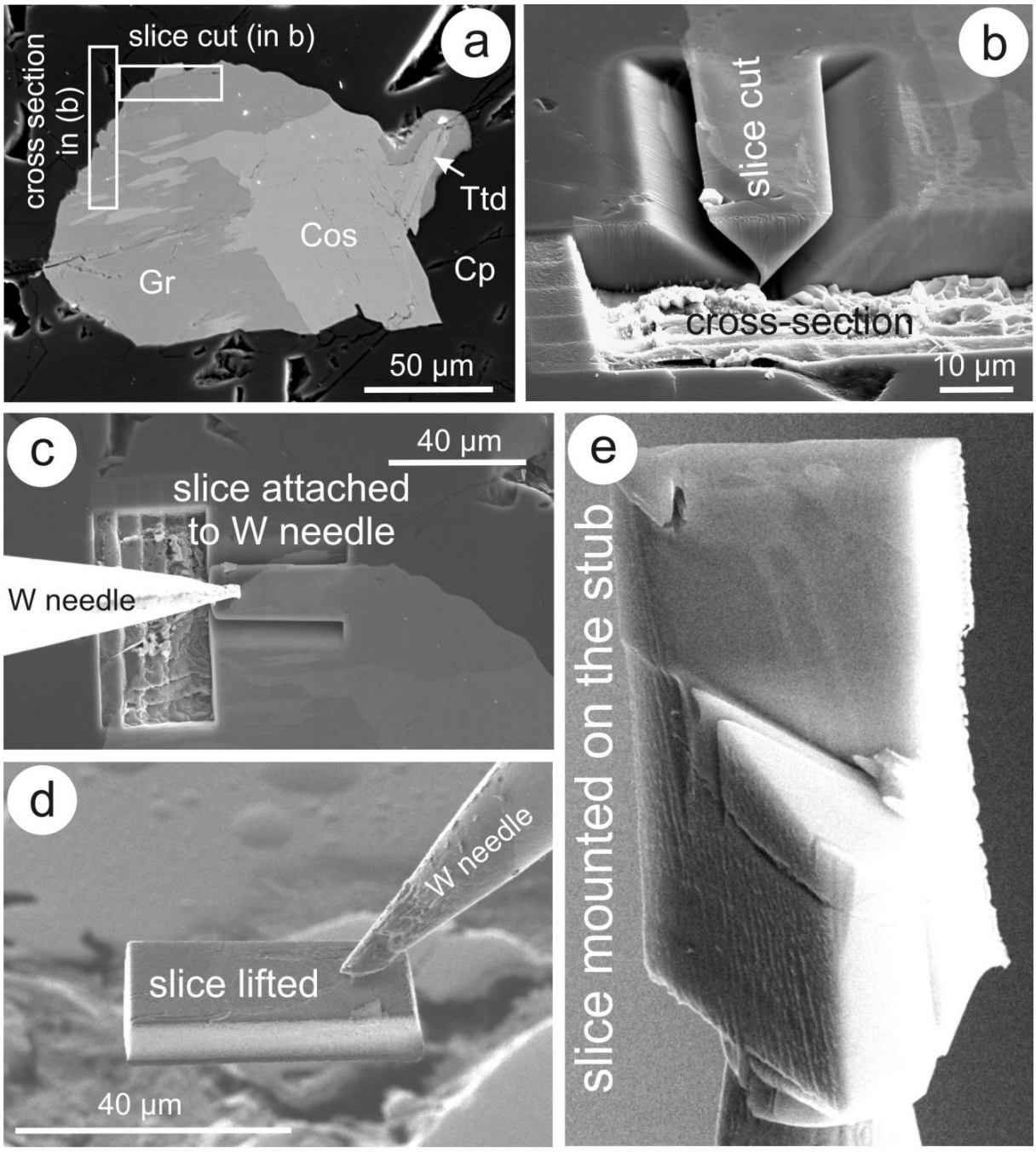

Ciobanu et al. Figure 2

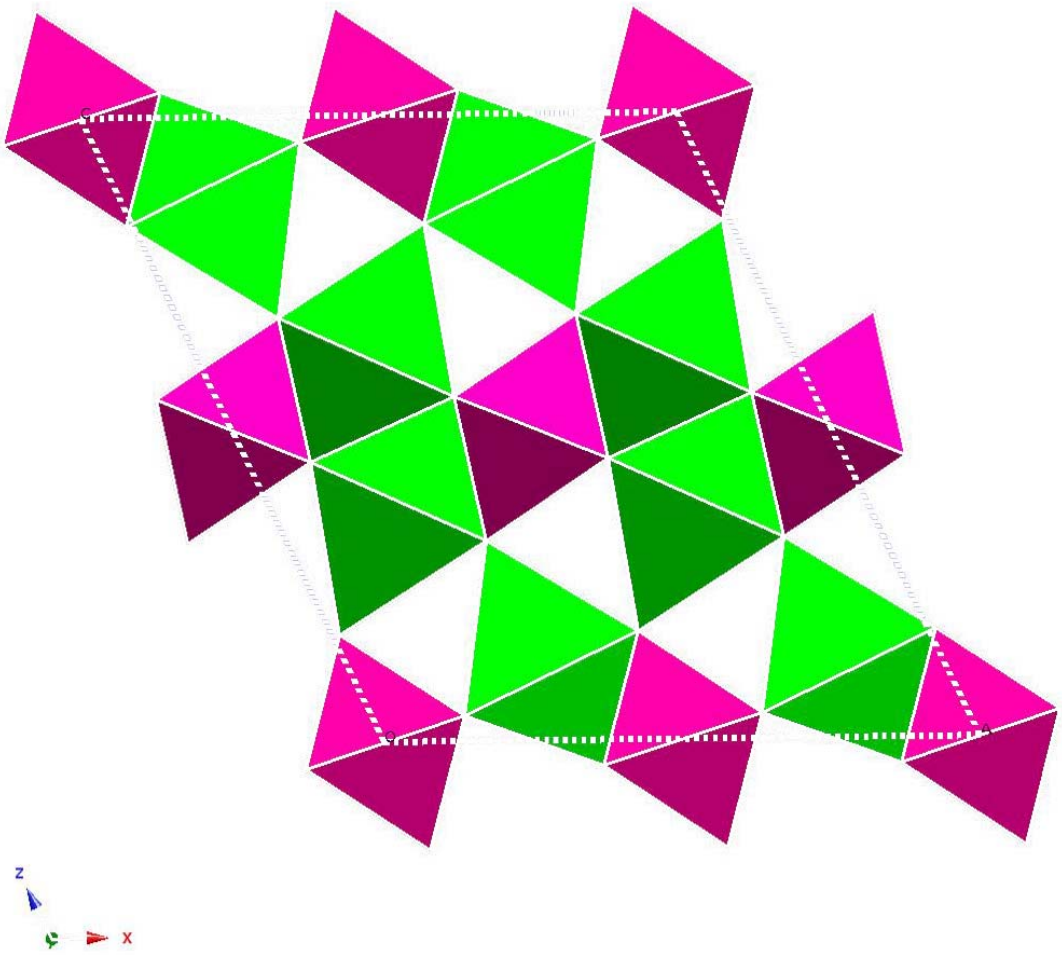

Figure 3.

Table 1. Electron probe microanalyses of gratianite.

Constituent	**Wt.%**	**Range**	**Stand. Dev.**	**Probe Standard**
Ag	0.02	0.00-0.48	0.10	Ag_2Te*
Cu	0.42	0.10-1.31	0.28	$CuFeS_2$
Pb	2.38	1.63-4.88	0.85	PbS*
Fe	2.92	1.39-3.62	0.56	FeS_2*
Mn	4.88	4.24-5.40	0.30	rhodonite
Cd	0.17	0.03-0.31	0.08	CdS*
Bi	67.76	65.28-68.70	0.79	Bi_2Se_3*
Sb	0.35	0.16-0.53	0.12	Sb_2S_3*
As	0.02	0.00-0.09	0.03	GaAs*
Te	0.15	0.00-1.13	0.25	Ag_2Te*
Se	0.15	0.05-0.30	0.07	Bi_2Se_3*
S	21.10	20.47-21.69	0.26	PbS*
Total	100.32	99.21-101.66		

*Synthetic standard

Table 2. Data collection and structure refinement details for grațianite.

Diffractometer	ADSC Quantum 315r detector
Radiation	synchrotron (λ = 0.71000 Å)
Temperature	298(2) K
Structural Formula	$Mn_{0.87}Bi_{2.075}S_4$
Space group	*C*2/*m*
Unit cell dimensions	*a* = 12.677(3) Å
	b = 3.9140(8) Å
	c = 14.758(3) Å
	β = 115.31(3)º
V	662.0(2) Å^3
Z	4
Absorption coefficient	57.844 mm^{-1}
Extinction coefficient	0.051(8)
F(000)	1039
θ range	1.53 to 29.52°
Index ranges	$-17 \le h \le 17$, $-5 \le k \le 5$, $-20 \le l \le 20$
Refls collected / unique	2716 / 878; R_{int} = 0.056
Reflections with $F > 4\sigma(F)$	878
Refinement method	Full-matrix least-squares on F^2
Parameters refined	48
GoF	1.342
Final *R* indices [$F_o > 4\sigma(F)$]	R_1 = 0.1035, wR_2 = 0.1041
R indices (all data)	R_1 = 0.2637, wR_2 = 0.2639
Largest diff. peak / hole	+6.62 / –4.68 *e*/A^3

*$R_{int} = \Sigma|F_o^2\text{-}F_o^2(\text{mean})|/\Sigma[F_o^2]$. GoF = $S = \{\Sigma[w(F_o^2 - F_c^2)^2]/(n-p)\}^{1/2}$. $R_1 = \Sigma||F_o|\text{-}|F_c||/\Sigma|F_o|$. $wR_2 = \{\Sigma[w(F_o^2 - F_c^2)^2]/\Sigma[w(F_o^2)^2]\}^{1/2}$; $w = 1/[\sigma^2(F_o^2) + (aP)^2 + bP]$ where *a* is 0, *b* is 394.6636 and *P* is $[2F_c^2 + \text{Max}(F_o^2,0)]/3$.

Table 3. Atom coordinates and displacement parameters (Å^2) for grațianite.

	x/*a*	*y*/*b*	*z*/*c*	U_{eq}	U_{11}	U_{22}	U_{33}	U_{23}	U_{13}	U_{12}	*Wyckoff position*
Bi1	0.22003(17)	0	0.36822(14)	0.0251(9)	0.0283(12)	0.0236(14)	0.0247(12)	0	0.0126(8)	0	8*i*
Bi2	0.35329(18)	0	0.13829(14)	0.0279(10)	0.0298(13)	0.0281(14)	0.0274(12)	0	0.0140(8)	0	8*i*
Mn3*	0	0	0.5	0.025(3)	0.021(4)	0.027(5)	0.029(4)	0	0.013(3)	0	2*b*
Mn4	0	0	0	0.027(2)	0.030(5)	0.031(7)	0.024(5)	0	0.015(4)	0	2*a*
S1	0.6537(10)	0	0.0422(9)	0.021(2)	0.017(5)	0.022(6)	0.024(5)	0	0.009(4)	0	8*i*
S2	0.0132(10)	0	0.1733(9)	0.022(2)	0.020(5)	0.020(6)	0.026(5)	0	0.011(4)	0	8*i*
S3	0.6044(9)	0	0.4492(8)	0.021(2)	0.014(4)	0.024(7)	0.020(5)	0	0.003(4)	0	8*i*
S4	0.8310(10)	0	0.3200(10)	0.023(2)	0.020(5)	0.027(7)	0.032(6)	0	0.019(4)	0	8*i*

*Mn3 occupancy = Mn 0.102, Fe 0.65, Pb 0.142, Cu 0.09 and Cd 0.016.

Table 4. Selected bond distances (Å) for graţianite.

Bi1	S3	2.663(11)	Bi2	S1	2.627(12)
	S4	2.678(7)	Bi2	S2	2.703(8)
	S4	2.678(7)	Bi2	S2	2.703(8)
	S2	2.950(12)	Bi2	S1	3.029(9)
	S3	2.984(9)	Bi2	S1	3.029(9)
	S3	2.984(9)	<Bi–S>		2.818
<Bi–S>		2.823			
Mn3	S4	2.604(13)	Mn4	S2	2.491(12)
Mn3	S4	2.604(13)	Mn4	S2	2.491(12)
Mn3	S3	2.644(8)	Mn4	S1	2.641(8)
Mn3	S3	2.644(8)	Mn4	S1	2.641(8)
Mn3	S3	2.644(8)	Mn4	S1	2.641(8)
Mn3	S3	2.644(8)	Mn4	S1	2.641(8)
<Mn–S>		2.631	<Mn-S>		2.591

Table 5. Calculated powder pattern for graţianite (CrystalDiffract). 2-Theta for Cu $K\alpha_1$ (1.54050 Å).

(N)	h	k	l	d(hkl) [Å]	2-Theta[°]	I/Imax
4	2	0	0	5.730	15.45	42.5
5	2	0	-2	5.720	15.48	42.0
6	2	0	1	4.600	19.28	30.3
7	2	0	-3	4.590	19.32	29.1
10	1	1	-1	3.703	24.01	18.4
11	2	0	2	3.644	24.41	53.8
12	2	0	-4	3.637	24.46	54.9
13	1	1	1	3.448	25.82	100.0
15	0	0	4	3.335	26.71	43.1
16	4	0	-2	3.169	28.13	18.8
17	4	0	-1	3.085	28.92	11.1
20	1	1	-3	3.062	29.14	51.7
21	2	0	3	2.954	30.23	9.6
25	3	1	-1	2.855	31.30	13.3
26	3	1	-2	2.855	31.31	63.6
27	3	1	0	2.734	32.73	16.4
28	3	1	-3	2.731	32.76	77.3
32	4	0	1	2.584	34.69	9.0
34	3	1	1	2.530	35.45	34.9
36	2	0	4	2.461	36.48	10.7
37	2	0	-6	2.457	36.54	11.4
39	1	1	-5	2.323	38.74	24.8
41	3	1	2	2.295	39.22	9.5
45	5	1	-2	2.122	42.58	16.0
58	1	1	5	2.036	44.47	30.8
60	6	0	-1	2.015	44.94	16.5
61	6	0	-5	2.013	45.00	17.1
62	5	1	0	1.978	45.84	16.9
64	0	2	0	1.957	46.36	27.2
72	5	1	-6	1.857	49.03	26.7
75	2	2	-2	1.852	49.17	17.3
83	1	1	-7	1.799	50.71	15.0
87	5	1	2	1.730	52.87	12.8
89	2	2	2	1.724	53.07	10.2
90	2	2	-4	1.723	53.10	10.9
91	0	2	4	1.688	54.31	9.7

Only peaks with I/Imax >9 are listed.

Table 6. Comparison of cell parameters for graţianite with selected analogue minerals and synthetic phases

Mineral/phase	**Formula**	***a* (Å)**	***b* (Å)**	***c* (Å)**	**Z**	**β (°)**	**Space group**	**Reference(s)**
Graţianite	$MnBi_2S_4$	12.677	3.914	14.758	4	115.313	*C2/m*	This study
Berthierite	$FeSb_2S_4$	11.44	14.12	3.76	4		*Pnam*	Bente and Edenharter (1990)
Garavellite	$FeBiSbS_4$	11.439	14.093	3.754	4		*Pnam*	Gregorio et al. (1979)
Clerite	$Mn(Sb,As)_2S_4$	11.47	14.36	3.81	4		*Pnam*	Murzin et al. (1996)
syn. $Mn_{0.7}Bi_{2.2}S_4$	$Mn_{0.7}Bi_{2.2}S_4$	12.869	3.955	14.771	4	116.691	*C2/m*	Lee et al. (1993)
syn. $Mn_{0.9}Bi_{2.06}Se_4$	$Mn_{0.9}Bi_{2.06}Se_4$	13.357	4.073	15.301	4	115.887	*C2/m*	Lee et al. (1993)
syn. $MnBi_2S_4$	$MnBi_2S_4$	12.7636	3.91614	14.7482	4	115.264	*C2/m*	Kurowski (2003)
syn. $MnSb_2S_4$	$MnSb_2S_4$	11.459	14.351	3.823		113.91	*Pnam*	Bente and Edenharter (1989)
syn. $MnSb_2S_4$	$MnSb_2S_4$	12.747	3.799	15.106	4	113.91	*C2/m*	Pfitzner and Kurowski (2000)
syn. $MnSb_2Se_4$	$MnSb_2Se_4$	13.319	4.001	14.967	4	115.1	*C2/m*	Kurowski (2003)
Grumiplucite	$HgBi_2S_4$	14.164	4.053	13.967	4	118.28	*C2/m*	Mumme and Watts (1980), Orlandi et al. (1998)
Kudriavite	$(Cd,Pb)Bi_2S_4$	13.095	4.0032	14.711	4	115.602	*C2/m*	Chaplygin et al. (2005), Balić-Žunić and Makovicky (2007)